Inorganic Chemistry
Article

Inorg. Chem. **2011**, *50*, 985–991 **985**
DOI: 10.1021/ic101618n

Reversible Single-Crystal-to-Single-Crystal Transformation and Highly Selective Adsorption Property of Three-Dimensional Cobalt(II) Frameworks

Zhi Su,[†] Min Chen,[†] Taka-aki Okamura,[‡] Man-Sheng Chen,[†] Shui-Sheng Chen,[†] and Wei-Yin Sun*[,†]

[†]*Coordination Chemistry Institute, State Key Laboratory of Coordination Chemistry, School of Chemistry and Chemical Engineering, Nanjing National Laboratory of Microstructures, Nanjing University, Nanjing 210093, China, and* [‡]*Department of Macromolecular Science, Graduate School of Science, Osaka University, Toyonaka, Osaka 560-0043, Japan*

Received August 9, 2010

A three-dimensional (3D) coordination polymer, $[Co_3(L)_2(BTEC)(H_2O)_2]\cdot 2H_2O$ [**1**, HL = 3,5-di(imidazol-1-yl)benzoic acid, H_4BTEC = 1,2,4,5-benzenetetracarboxylic acid], with **tfz-d** topology has been hydrothermally synthesized. The framework of **1** has high thermal stability and exhibits single-crystal-to-single-crystal (SCSC) transformations upon removing and rebinding the noncoordinated and coordinated water molecules. X-ray crystallographic analyses revealed that the coordination geometry of Co(II) changes from octahedral to square pyramid upon dehydration, accompanying the appearance of one-dimensional (1D) open channels with dimensions of 2.0 × 2.8 Å. The dehydrated form $[Co_3(L)_2(BTEC)]$ (**2**) exhibits highly selective adsorption of water molecules over N_2, CH_3OH, and CH_3CH_2OH, which could be used as sensors for water molecules. Furthermore, the magnetic properties of **1** and **2** were investigated, showing the existence of ferromagnetic interaction between the Co(II) atoms within the trinuclear subunit.

Introduction

Recently, the design and construction of porous coordination polymers (PCPs) with large surface area have been of great interest due to their potential applications in gas storage, separation, ion exchange, catalysis, sensors, and magnetism.[1] Multicarboxylate ligands were widely used as bridging linkers in the construction of PCPs due to the high thermal and chemical stabilities of polycarboxylate-metal fragments.[2] Particularly, some reported flexible porous frameworks display unique dynamic behaviors in response to external stimuli with reversible changes of their structures and properties which are called single-crystal-to-single-crystal (SCSC) or single-crystal-to-amorphous transformations,[3] while the others with switchable guest molecules are unstable after the removal of the guest, which leads to the collapse of the frameworks.[4] It has been demonstrated that the SCSC transformation is highly desirable and opens routes to the systematic study of gas storage, separation, and solid state reaction, since it allows direct visualization of how the crystal structure is changing during the transformation process and of the location and orientation of guest molecules in the voids, where single crystallographic analysis, as the most direct evidence of this transformation, can supply enough structural information.[5] However, the exploration via SCSC transformations is uncommon so far.

*To whom correspondence should be addressed. Fax: +86-25-83314502. E-mail: sunwy@nju.edu.cn.

(1) (a) Llewellyn, P. L.; Horcajada, P.; Maurin, G.; Devic, T.; Rosenbach, N.; Bourrelly, S.; Serre, C.; Vincent, D.; Loera-Serna, S.; Filinchuk, Y.; Férey, G. *J. Am. Chem. Soc.* **2009**, *131*, 13002. (b) Clegg, J. K.; Iremonger, S. S.; Hayter, M. J.; Southon, P. D.; Macquart, R. B.; Duriska, M. B.; Jensen, P.; Turner, P.; Jolliffe, K. A.; Kepert, C. J.; Meehan, G. V.; Lindoy, L. F. *Angew. Chem., Int. Ed.* **2010**, *49*, 1075. (c) Abrahams, B. F.; Grannas, M. J.; Hudson, T. A.; Robsen, R. *Angew. Chem., Int. Ed.* **2010**, *49*, 1087. (d) Cheon, Y. E.; Suh, M. P. *Chem. Commun.* **2009**, 2296. (e) Lin, J. B.; Zhang, J. P.; Zhang, W. X.; Xue, W.; Xue, D. X.; Chen., X. M. *Inorg. Chem.* **2009**, *48*, 6652.

(2) (a) Han, Z. B.; Zhang, G. X.; Zeng, M. H.; Yuan, D. Q.; Fang, Q. R.; Li, J. R.; Ribas, J.; Zhou, H. C. *Inorg. Chem.* **2010**, *49*, 769. (b) Koh, K.; Wong-Foy, A. G.; Matzger, A. J. *J. Am. Chem. Soc.* **2009**, *131*, 4184. (c) Wang, X. L.; Liu, G. C.; Zhang, J. X.; Chen, Y. Q.; Lin, H. Y.; Zheng, W. Y. *Dalton Trans.* **2009**, 7347. (d) Zhang, Y. B.; Zhang, W. X.; Feng, F. Y.; Zhang, J. P.; Chen, X. M. *Angew. Chem., Int. Ed.* **2009**, *48*, 5287. (e) Rueff, J. M.; Barrier, N.; Boudin, S.; Dorcet, V.; Caignaert, V.; Boullay, P.; Hix, G. B.; Jaffrès, P. A. *Dalton Trans.* **2009**, 10614.

(3) (a) Allan, P. K.; Xiao, B.; Teat, S. J.; Knight, J. W.; Morris, R. E. *J. Am. Chem. Soc.* **2010**, *132*, 3605. (b) Zeng, M. H.; Wang, Q. X.; Tan, Y. X.; Hu, S.; Zhao, H. X.; Long, L. S.; Kurmoo, M. *J. Am. Chem. Soc.* **2010**, *132*, 2561. (c) Maji, T. K.; Mostafa, G.; Matsuda, R.; Kitagawa, S. *J. Am. Chem. Soc.* **2005**, *127*, 17152. (d) Cai, Y. P.; Zhou, X. X.; Zhou, Z. Y.; Zhu, S. Z.; Thallapally, P. K.; Liu, J. *Inorg. Chem.* **2009**, *48*, 6341. (e) Braga, D.; Maini, L.; Mazzeo, P. P.; Ventura, B. *Chem.—Eur. J.* **2010**, *16*, 1553.

(4) (a) Chen, X. D.; Zhao, X. H.; Chen, M.; Du, M. *Chem.—Eur. J.* **2009**, *15*, 12974. (b) Ene, C. D.; Madalan, A. M.; Maxim, C.; Jurca, B.; Avarvari, N.; Andruh, M. *J. Am. Chem. Soc.* **2009**, *131*, 4586. (c) Maji, T. P.; Uemura, K.; Chang, H. C.; Matsuda, R.; Kitagawa, S. *Angew. Chem., Int. Ed.* **2004**, *43*, 3269. (d) Sengupta, O.; Song, Y.; Mukherjee, P. S. *Dalton Trans.* **2009**, 10343. (e) Cheng, X. N.; Zhang, W. X.; Chen, X. M. *J. Am. Chem. Soc.* **2007**, *129*, 15738.

(5) (a) Nouar, F. N.; Eubank, J. F.; Bousquet, T.; Wojtas, L.; Zaworotko, M. J.; Eddaoudi, M. *J. Am. Chem. Soc.* **2008**, *130*, 1833. (b) Lan, Y. Q.; Li, S. L.; Shao, K. Z.; Wang, X. L.; Du, D. Y.; Su, Z. M.; Wang, D. J. *Cryst. Growth Des.* **2008**, *8*, 3940. (c) Zhai, Q. G.; Wu, X. Y.; Chen, S. M.; Zhao, Z. G.; Lu, C. Z. *Inorg. Chem.* **2007**, *46*, 5046.

Published on Web 01/10/2011

During our efforts toward the rational design and synthesis of PCPs with mixed imidazoles containing ligands and carboxylic acid,[6] we have prepared a new Co(II) complex, $[Co_3(L)_2(BTEC)(H_2O)_2]\cdot 2H_2O$ [**1**, HL = 3,5-di(imidazol-1-yl)-benzoic acid, H_4BTEC = 1,2,4,5-benzenetetracarboxylic acid], through the hydrothermal method: the complex has a three-dimensional (3D) host framework with the inclusion of water molecules as the guests. Remarkably, the reversible de/rehydrated SCSC transformation was found in the heating and after standing in the air. Interestingly, $[Co_3(L)_2(BTEC)]$ (**2**) exhibits highly selective adsorption of the water molecules over N_2, CH_3OH, and CH_3CH_2OH, which can be used as sensors for water molecules. Furthermore, the magnetic properties of **1** and **2** were investigated.

Experimental Section

All commercially available chemicals are of reagent grade and were used as received without further purification. The ligand HL was prepared according to the procedures reported previously.[7] Elemental analyses of C, H, and N were performed on a Perkin-Elmer 240C elemental analyzer at the analysis center of Nanjing University. Infrared spectra (IR) were recorded on a Bruker Vector22 FT-IR spectrophotometer using KBr pellets. Thermogravimetric analyses (TGA) were performed on a simultaneous SDT 2960 thermal analyzer under nitrogen at a heating rate of 10 °C min^{-1}. Variable temperature powder X-ray diffraction (PXRD) analyses were performed on a Shimadzu XRD-6000 X-ray diffractometer with Cu Kα (λ = 1.5418 Å) radiation. Solid state UV−visible spectra were measured in diffuse reflectance mode on a Shimadzu UV3600 spectrophotometer coupled to a MPC-3100 unit equipped with an integrating sphere coated with $BaSO_4$. The magnetic measurements in the temperature range of 1.8 to 300 K were carried out on a Quantum Design MPMS7 SQUID magnetometer in a field of 2000 Oe. Diamagnetic corrections were made with Pascal's constants for all samples. Nitrogen (N_2), methanol (CH_3OH), ethanol (CH_3CH_2OH), and H_2O sorption experiments were carried out on a Belsorp-max volumetric gas sorption instrument. The sample was dried by using the "outgas" function of the surface area analyzer for 10 h at 160 °C to remove the H_2O molecules.

Preparation of $[Co_3(L)_2(BTEC)(H_2O)_2]\cdot 2H_2O$ (1). A mixture of $CoCl_2\cdot 6H_2O$ (57.4 mg, 0.2 mmol), HL (25.4 mg, 0.1 mmol), H_4BTEC (25.4 mg, 0.1 mmol), NaOH (20.0 mg, 0.5 mmol), and H_2O (10 mL) was sealed in a 16 mL Teflon lined stainless steel container and heated at 210 °C for 3 d. Complex **1** was isolated in red block crystalline form by filtration and washed by water and ethanol several times with a yield of 63%. Anal. Calcd for $C_{36}H_{28}Co_3N_8O_{16}$ (%): C, 43.00; H, 2.81; N, 11.14. Found: C, 43.11; H, 2.75; N, 11.10. IR (KBr, cm^{-1}): 3448(s, br), 1651(s), 1616(m), 1582(s), 1514(s), 1478(m), 1418(s), 1376(m), 1323(s), 1234(w), 1073(s), 935(w), 905(w), 843(m), 787(w), 738(m), 656(m), 522(w).

Preparation of $[Co_3(L)_2(BTEC)]$ (2). Complex **2** was obtained by heating the crystal sample of **1** at 160 °C for 2 h. Anal. Calcd for $C_{36}H_{20}Co_3N_8O_{12}$ (%): C, 46.32; H, 2.16; N; 12.00. Found: C, 46.30; H, 2.13; N; 12.08. IR (KBr, cm^{-1}): 1651(s), 1617(m), 1581(s), 1513(s), 1478(m), 1417(s), 1375(m), 1324(s), 1234(w), 1073(s), 935(w), 908(w), 843(m), 787(w), 738(m), 656(m), 522(w).

Table 1. Crystal Data and Structure Refinements for Complexes **1** and **2**

	1	**2**
empirical formula	$C_{36}H_{28}Co_3N_8O_{16}$	$C_{36}H_{20}Co_3N_8O_{12}$
fw	1005.45	933.39
temp/K	293	433
cryst syst	triclinic	triclinic
space group	$P\bar{1}$	$P\bar{1}$
a/Å	8.550(4)	8.683(6)
b/Å	10.077(3)	9.849(6)
c/Å	11.255(4)	10.927(7)
α/deg	77.672(13)	71.60(2)
β/deg	73.974(17)	73.81(3)
γ/deg	88.701(17)	86.83(3)
V (Å^3)	909.8(6)	851.0(10)
Z	1	1
Dc (g cm^{-3})	1.835	1.821
F(000)	509	469
θ range/deg	3.1 - 27.5	3.1 - 27.5
reflns collected	8656	8033
independent reflns	4138	3875
goodness of fit	1.082	1.102
$R_1{}^a$ ($I > 2\sigma(I)$)	0.0312	0.0382
$wR_2{}^b$ ($I > 2\sigma(I)$)	0.0813	0.1015

$^a R_1 = \sum||F_o| - |F_c||/\sum|F_o|$. $^b wR_2 = |\sum\sum w(|F_o|^2 - |F_c|^2)|/\sum|w(F_o)^2|^{1/2}$, where $w = 1/[\sigma^2(F_o^2) + (aP)^2 + bP]$. $P = (F_o^2 + 2F_c^2)/3$.

Rehydration of 2. Standing the crystal sample of **2** in the air for several hours gave rise to the rehydrated complex **1′**.

Single Crystal X-Ray Structural Determinations. The crystallographic data for **1** and **2** were collected on a Rigaku RAXIS-RAPID imaging plate diffractometer at 293 and 433 K, respectively, with graphite-monochromated Mo Kα radiation (λ = 0.71075 Å). The structures were solved by direct methods with SIR92 and expanded using Fourier techniques.[8,9] All non-hydrogen atoms were refined anisotropically using the full-matrix least-squares method on F^2. Hydrogen atoms of the ligands in **1** and **2** were generated geometrically, and those of water molecules (O7, O8) in **1** were located directly. All calculations were carried out on an SGI workstation using the teXsan crystallographic software package of Molecular Structure Corporation.[10] The crystallographic data collections for **1′** were carried out on a Bruker Smart Apex CCD area-detector diffractometer with graphite-monochromated Mo Kα radiation (λ = 0.71073 Å) at 293 K using the ω-scan technique. The diffraction data were integrated using the *SAINT* program,[11] which was also used for the intensity corrections for the Lorentz and polarization effects. Semiempirical absorption correction was applied using the *SADABS* program.[12] The structure was solved by direct methods, and all non-hydrogen atoms were refined anisotropically on F^2 with the full-matrix least-squares technique using the *SHELXL-97* crystallographic software package.[13] All of the hydrogen atoms of ligands were generated geometrically, those of water molecule (O8) were located directly, and those of O7 were not found. All calculations were performed on a personal computer with the SHELXL-97

(6) (a) Su, Z.; Cai, K.; Fan, J.; Chen, S. S.; Chen, M. S.; Sun, W. Y. *CrystEngComm* **2010**, *12*, 100. (b) Su, Z.; Bai, Z. S.; Xu, J.; Okamura, T.-a.; Liu, G. X.; Chu, Q.; Wang, X. F.; Sun, W. Y.; Ueyama, N. *CrystEngComm* **2009**, *11*, 873. (c) Su, Z.; Fan, J.; Okamura, T.-a.; Chen, M. S.; Chen, S. S.; Sun, W. Y.; Ueyama, N. *Cryst. Growth Des.* **2010**, *10*, 1911. (d) Su, Z.; Bai, Z. S.; Fan, J.; Xu, J.; Sun, W. Y. *Cryst. Growth Des.* **2009**, *9*, 5190.

(7) Fan, J.; Gan, L.; Kawaguchi, H.; Sun, W. Y.; Yu, K. B.; Tang, W. X. *Chem.—Eur. J.* **2003**, *9*, 3965.

(8) SIR92: Altomare, A.; Burla, M. C.; Camalli, M.; Cascarano, M.; Giacovazzo, C.; Guagliardi, A.; Polidori, G. *J. Appl. Crystallogr.* **1994**, *27*, 435.

(9) Beurskens, P. T.; Admiraal, G.; Beurskens, G.; Bosman, W. P.; Gelder, R. de; Israel, R. Smits, J. M. M. DIRDIF94: The DIRDIF-94 Program System, Technical Report of the Crystallography Laboratory, University of Nijmegen, The Netherlands, 1994.

(10) *teXsan*; Molecular Structure Corporation: The Woodlands, TX, 1999.

(11) *SAINT*, version 6.2; Bruker AXS, Inc.: Madison, WI, 2001.

(12) Sheldrick, G. M. *SADABS*; University of Göttingen: Göttingen, Germany.

(13) Sheldrick, G. M. *SHELXTL*, version 6.10; Bruker Analytical X-ray Systems: Madison, WI, 2001.

Table 2. Selected Bond Lengths [Å] and Bond Angles [deg] for Complexes **1** and **2**

1[a]

Co1−O1	2.0612(13)	Co1−O5#1	2.0538(14)
Co1−O3#2	2.1111(14)		
Co2−O3	2.1535(18)	Co2−O6#1	2.0697(14)
Co2−N12	2.1208(17)	Co2−O1#2	2.0959(14)
Co2−O7	2.1138(17)	Co2−N32#3	2.1164(17)
O1−Co1−O3	95.42(5)	O3−Co1−O3#2	180.00
O1−Co1−O5#1	87.58(6)	O5#1−Co1−O5#4	180.00
O1−Co1−O1#2	180.00	O1#2−Co1−O5#1	92.42(6)
O3−Co1−O5#1	88.29(6)	O3#2−Co1−O5#1	91.71(6)
O1#2−Co1-O3	84.58(5)		
O3−Co2−N12	92.02(6)	O6#1−Co2−N12	176.11(6)
O3−Co2−O6#1	89.45(6)	O1#2−Co2−N12	89.46(6)
O1#2−Co2−O3	81.53(5)	N12−Co2−N32#3	89.73(7)
O3−Co2−N32#3	177.84(5)	O1#2−Co2−O6#1	94.32(5)
O6#1−Co2−O7	91.13(6)	O3−Co2−O7	85.98(7)
O1#2−Co2−O7	166.31(7)	O7−Co2−N12	85.38(7)
O7−Co2−N32#3	95.42(7)	O6#1−Co2−N32#3	88.88(7)
O1#2−Co2−N32#3	97.24(6)		

2[a]

Co1−O1	2.0401(18)	Co1−O5#1	2.1220(19)
Co1−O3	2.0710(19)		
Co2−O3	2.1535(18)	Co2−O1#2	2.076(2)
Co2−O6#1	1.982(2)	Co2−N32#3	2.127(2)
Co2−N12	2.043(2)		
O1−Co1−O3	96.56(7)	O3−Co1−O5#1	86.33(8)
O1−Co1−O5#1	89.64(8)	O3−Co1−O3#2	180.00
O1−Co1−O1#2	180.00	O5#1−Co1−O5#4	180.00
O1−Co1−O3#2	83.44(7)	O1#2−Co1−O5#1	90.36(8)
O3#2−Co1−O5#1	93.67(8)		
O3−Co2−N12	89.90(9)	O1#2−Co2-N12	99.22(8)
O3−Co2−O6#1	92.46(9)	N32#3−Co2-N12	86.94(10)
O1#2−Co2−O3	80.59(7)	O1#2−Co2−O6#1	101.35(8)
O3−Co2−N32#3	174.72(7)	O6#1−Co2−N32#3	91.98(9)
O6#1−Co2−N12	159.41(9)	O1#2−Co2−N32#3	95.74(8)

[a] Symmetric transformations used to generate equivalent atoms for **1**−**2**. #1: $1+x, y, -1+z$. #2: $2-x, -y, -z$. #3: $2-x, 1-y, 1-z$. #4: $1-x, -y, 1-z$.

crystallographic software package. In addition, the crystallographic data for **1**, **2**, and **1′** can be collected from the same single crystal, showing reversible dehydration and rehydration cycles. Details of the crystal parameters, data collection, and refinements are summarized in Table 1 for **1** and **2** and Table S1 (Supporting Information) for **1′**, and selected bond lengths and angles for **1**, **2**, and **1′** are listed in Tables 2 and S2 (Supporting Information), respectively. Further details are provided in the Supporting Information.

Results and Discussion

Crystal Structure of Complex 1. Single crystal X-ray diffraction analysis revealed that complex **1** crystallizes in the triclinic $P\bar{1}$ space group (Table 1). In the asymmetric unit of **1**, there are two different Co(II) atoms (Co1, Co2), one of which (Co1) is sitting on an inversion center; one L^- and half a molecule of $BTEC^{4-}$; and one coordinated and one free water molecule. Each Co1 with slightly distorted octahedral coordination geometry is six-coordinated by four oxygen atoms (O1, O3, O1A, O3A) from two distinct $BTEC^{4-}$ ligands and other two (O5B, O5D) from two different L^- ligands (Figure 1a). The average bond length of Co1−O is 2.07 Å. Each Co2 also with distorted octahedral coordination geometry is six-coordinated by four oxygen atoms, three of which (O1A, O3, O6B) are from three distinct $BTEC^{4-}$ ligands and one of which (O7) is from a terminal water molecule, and two nitrogen atoms (N12, N32C) from two different L^- ligands as shown in Figure 1a. The average Co2−O bond length is 2.11 Å, and the Co2−N bond distances are 2.1208(17) and 2.1164(17) Å (Table 2). It is interesting to find that the Co1 links two Co2 atoms by sharing two edges of a coordination octahedron to form a $Co_3(OCO)_6$ linear trinuclear secondary building unit (SBU) with a Co1···Co2 distance of 3.08 Å (Scheme 1).

On the other hand, each L^- ligand links three SBUs using its two imidazole groups and a carboxylate in the μ_2-η^1:η^1-bidentate bridging mode to form an infinite two-dimensional (2D) network (Figure S1, Supporting Information). The 2D layer can be simplified to a (3,6)-connected **kgd** net with SBU−SBU distances of 12.11, 13.36, and 16.64 Å, respectively, if the SBU and L^- ligand are considered a six-connected node and three-connector, respectively (Scheme S1 and Figure S1, Supporting Information).[14] Each $BTEC^{4-}$ ligand connects two SBUs using its four μ_2-η^2:η^0-bridging carboxylate groups to form an infinite one-dimensional (1D) chain with a SBU−SBU distance of 8.55 Å (Scheme S1, Figure S2, Supporting Information). The 2D networks are further connected by $BTEC^{4-}$ ligands to result in the formation of a three-dimensional (3D) framework of **1** (Figure 1b). Therefore, each SBU is eight-connected by six L^-'s in the 2D network and two SBUs via the $BTEC^{4-}$ ligands. The 3D framework of **1** can be viewed as a binodal (3,8)-connected net, referred to as the **tfz-d** net with a Point (Schläfli) symbol of $(4^3)_2(4^6\cdot6^{18}\cdot8^4)$ (Figure 1c).[15]

The most striking feature of complex **1** is the existence of open channels running along the *c* axis with effective dimensions of ca. 2.4 × 3.4 Å. Four water molecules (two coordinated and two noncoordinated) per formula unit are located within the channels (Figure 1d) and are involved in extensive hydrogen-bonding interactions with the framework (Table S3, Supporting Information). PLATON analysis suggests that the channels occupy 6.5% of the total volume [59.2 $Å^3$/909.8(6) $Å^3$].[16]

Thermal Stability and Powder X-ray diffraction (PXRD). To examine the thermal stabilities of complexes **1** and **2**, thermogravimetric analyses (TGA) and PXRD were carried out (Figures S3 and S4, Supporting Information). A two-step weight loss of complex **1** was observed in the temperature range of 40−200 °C, namely, 3.41% between 40 and 135 °C and 3.73% between 135 and 200 °C, which is ascribed respectively to the loss of noncoordinated and coordinated water molecules (total calcd, 7.16%), to give the dehydrated form **2**. The further weight loss in the range of 330−600 °C was attributed to the decomposition of the framework to form CoO as a final product (observed, 22.96%; calcd, 21.50%). No obvious weight loss

(14) (a) Hu, B. W.; Zhao, J. P.; Yang, Q.; Hu, T. L.; Du, W. P.; Bu, X. H. *J. Solid State Chem.* **2009**, *182*, 2918. (b) Kostakis, G. E.; Mondal, K. C.; Anson, C. E.; Powell, A. K. *Polyhedron* **2010**, *29*, 24. (c) Jiang, T.; Zhang, X. M. *Cryst. Growth Des.* **2008**, *8*, 3077.

(15) (a) Luo, F.; Che, Y. X.; Zheng, J. M. *Cryst. Growth Des.* **2008**, *8*, 2006. (b) Wang, S. N.; Xing, H.; Li, Y. Z.; Bai, J. F.; Pan, Y.; Scheer, M.; You, X. Z. *Eur. J. Inorg. Chem.* **2006**, 3041. (c) Xu, G. J.; Zhao, Y. H.; Shao, K. Z.; Lan, Y. Q.; Wang, X. L.; Su, Z. M.; Yan, L. K. *CrystEngComm* **2009**, *11*, 1842. (d) Garibay, S. J.; Stork, J. R.; Wang, Z. Q.; Cohen, S. M.; Telfer, S. G. *Chem. Commun.* **2007**, 4881. (e) Feng, Y.; Yang, E. C.; Fu, M.; Zhao, X. J. *Z. Anorg. Allg. Chem.* **2010**, *636*, 253.

(16) Spek, A. L. *J. Appl. Crystallogr.* **2003**, *36*, 7.

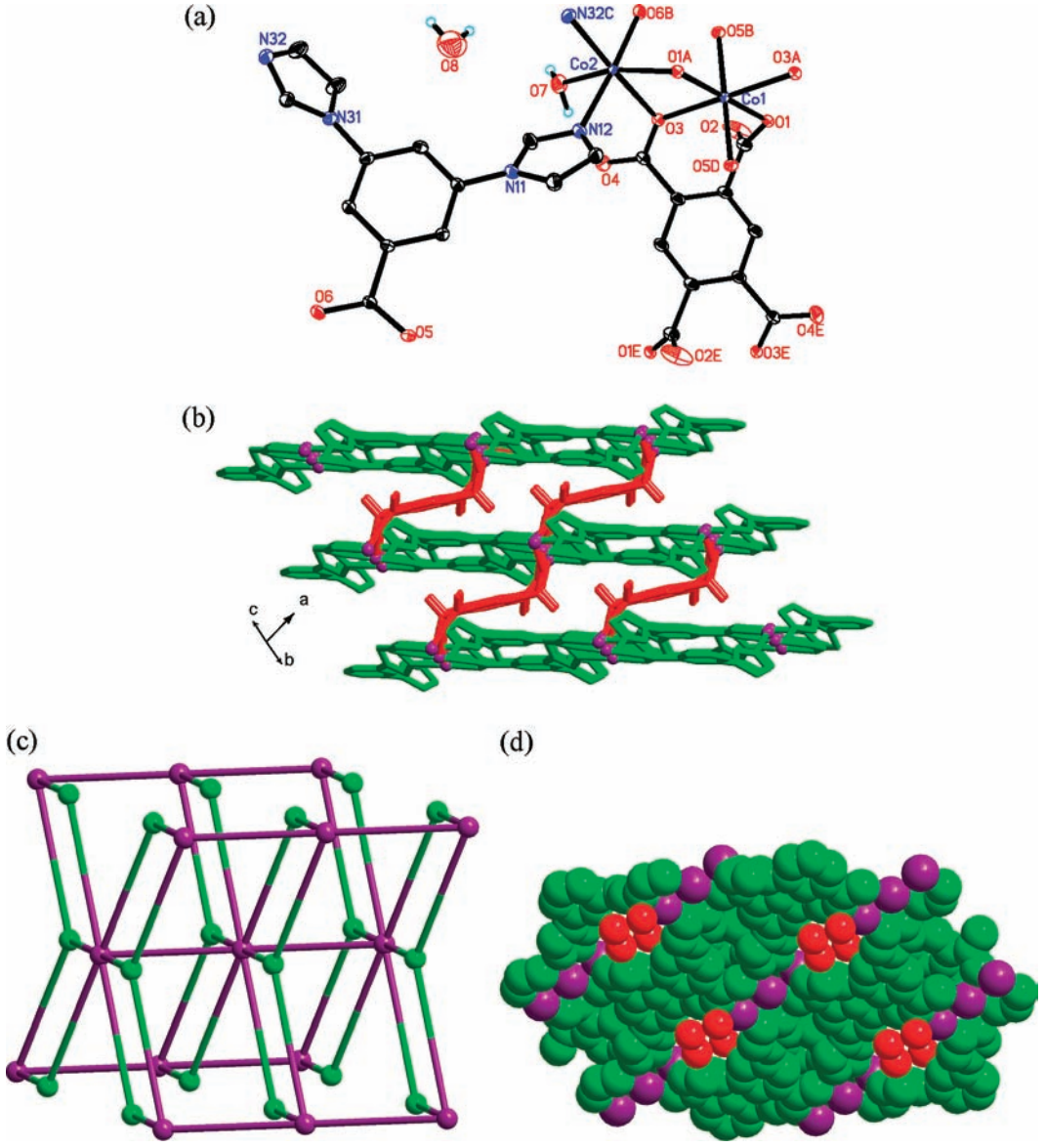

Figure 1. (a) The coordination environment of Co(II) atoms in **1** with the ellipsoids drawn at the 30% probability level. The hydrogen atoms of the ligands were omitted for clarity. (b) The 3D framework of complex **1**. (c) The (3,8)-connected **tfz-d** net of **1**. (d) Space-filling view of the 3D framework of **1** along the *c* axis, where the water molecules are represented by the red balls.

Scheme 1. View of the Trinuclear SBU in **1**

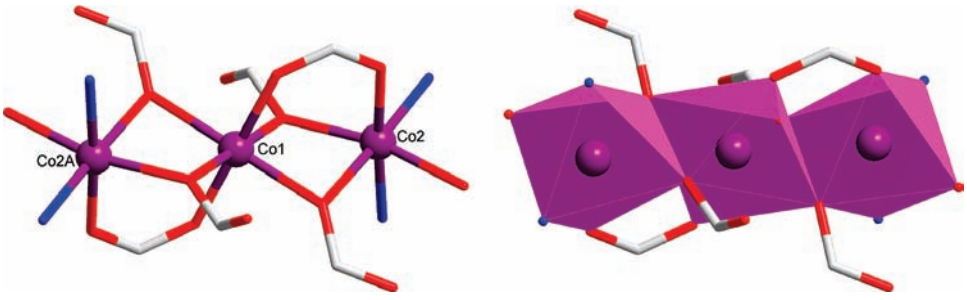

of **2** was observed at the starting temperature, and the framework decomposition occurred in the temperature range of 330−620 °C to give the final CoO product (observed, 23.86%; calcd, 23.15%).

Figure S4 (Supporting Information) shows the PXRD patterns of the as-synthesized **1** in the range of 25−350 °C. It is clear that the diffraction profiles below 330 °C are almost the same, indicating that the framework is stable under this temperature and the crystal lattice remains intact after removal of the water molecules. However, the sample became amorphous when the temperature was increased to 350 °C, as shown by the absence of

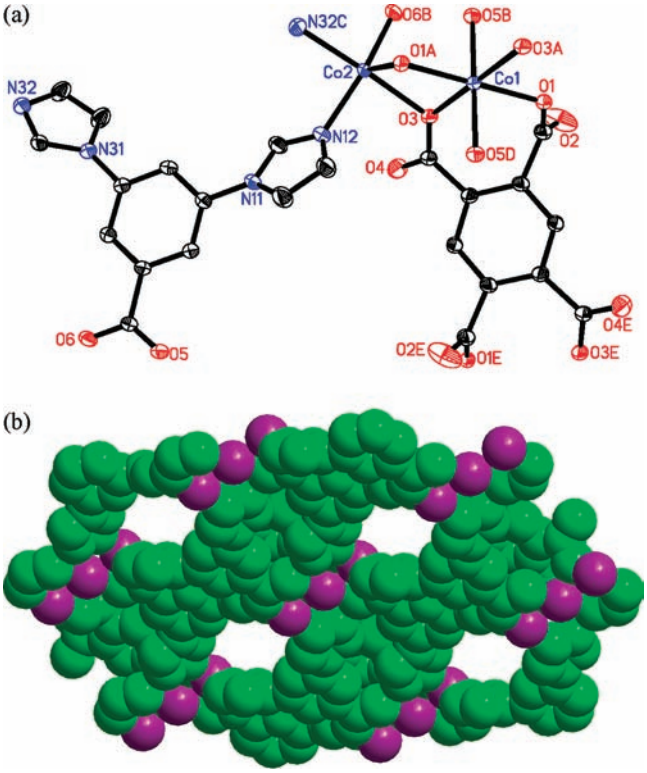

Figure 2. (a) The coordination environment of Co(II) atoms in **2** with the ellipsoids drawn at the 30% probability level. The hydrogen atoms of ligands were omitted for clarity. (b) Space-filling view of the 3D framework of **2** along *c* axis.

diffraction peaks in the PXRD pattern. It can be concluded that **1** has excellent thermal stability.

Reversible Single-Crystal-to-Single-Crystal Transformations upon Dehydration and Rehydration (1−2−1′). The openness of the channels makes it possible to remove the uncoordinated and coordinated water molecules from **1**. When crystals of **1** were heated at 160 °C for 2 h to remove the water molecules, the dehydrated product, $[Co_3(L)_2(BTEC)]$ (**2**), was obtained with retention of the single crystallinity, accompanying a color change from red to dark-violet (solid state UV−visible spectra of **1** and **2** shown in Figure S5, Supporting Information). Single crystal X-ray diffraction of **2** confirms that the framework structure and packing mode of **1** are retained and the space previously occupied by water molecules becomes devoid of any appreciable electron density (Figure 2a and b). Although the crystal system and space group remain unchanged (triclinic, $P\bar{1}$), the coordination geometry of Co2 changed from octahedral to square pyramid, where the bond angle of O6#1−Co2−N12 [symmetric code: $1+x$, y, $-1+z$] decreased from 176.11(6) to 159.41(9)° and the bond lengths of Co2−O6#1 and Co2−N12 decreased from 2.0697(14) and 2.1208(17) to 1.982(2) and 2.043(2) Å, respectively (Figure 2a, Table 2). The void volume occupied 3.8% of the total crystal volume for **2** [32.7/851.0(10) Å^3] with dimensions of 2.0 × 2.8 Å for the open channels along the *c* axis, which is obviously smaller than that in **1** (2.4 × 3.4 Å). Moreover, the unit-cell volume is decreased from 909.8(6) for **1** to 851.0(10) Å^3 for **2**, decreasing the volume by about 6.5%. In addition, the distance between Co1 and Co2 within the SBU decreased from 3.08 to 3.04 Å.

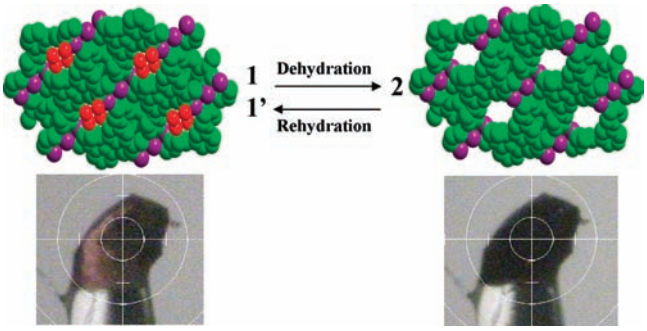

Figure 3. Reversible single-crystal-to-single-crystal transformations of dehydration and rehydration between **1** and **2**.

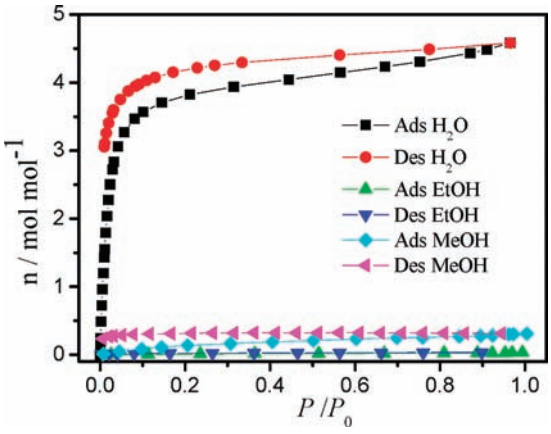

Figure 4. Solvent vapor adsorption and desorption isotherms of **2** at 298 K, which shows highly selective adsorption of H_2O vapor over other organic solvents.

Furthermore, the dehydrated process can be reversed by exposing the dehydrated sample to the air or water vapor or through the immersion of **2** into water at room temperature for several hours. The crystallographic investigation confirmed that the framework structure of the rehydrated sample **1′** is the same as that of **1**, accompanying a return of the original color (Figure 3). Thus, the Co2 atom provides a coordination site for the water molecule and returns to the octahedral coordination geometry. In conclusion, the SCSC transformations between **1**−**2**−**1′** involve dynamic motions altering the coordination geometry of Co(II) from/to an octahedron to/from a square pyramid as well as the shrinkage/expansion of pore deformation.

Sorption Properties. On the basis of the well-defined porous structure of the dehydrated product **2**, the adsorption isotherms for different solvents (H_2O, CH_3OH, CH_3CH_2OH) at 298 K as well as N_2 at 77 K were measured. The amount of water vapor uptaken increases abruptly at the beginning and reaches approximately 4.59 H_2O molecules per formula unit at 1.0 atm, which presents a typical type-I curve, indicating there is diffusion of water molecules into the channels (Figure 4).[17] The observed hysteresis between the adsorption−desorption

(17) (a) Zhong, D. C.; Lin, J. B.; Lu, W. G.; Jiang, L.; Lu, T. B. *Inorg. Chem.* **2009**, *48*, 8656. (b) Choi, H. S.; Suh, M. P. *Angew. Chem., Int. Ed.* **2009**, *48*, 6865. (c) Zhu, A. X.; Lin, J. B.; Zhang, J. P.; Chen, X. M. *Inorg. Chem.* **2009**, *48*, 3882. (d) Chen, M. S.; Bai, Z. S.; Okumura, T.-a.; Su, Z.; Chen, S. S.; Sun, W. Y.; Ueyama, N. *CrystEngComm* **2010**, *12*, 1935.

curves may be attributed to the intercrystalline voids.[18] It should be noticed that only surface adsorption has occurred in the CH_3OH and CH_3CH_2OH vapor adsorption measurements, and the isotherms are characteristic type-II curves. Namely, complex **2** has a highly selective adsorption of H_2O over CH_3OH and CH_3CH_2OH, which should be ascribed to the different kinetic diameters of these molecules.[19]

Obviously, the N_2 gas is different from the solvent vapor, which has no ability to bend or rotate molecular linkages. The resulting N_2 adsorption isotherm is shown in Figure S6 (Supporting Information), which is a characteristic type-H3 sorption behavior.[20] Furthermore, hysteresis was also observed between the adsorption−desorption curves. The result implies that only surface adsorption has occurred, indicating that nitrogen molecules cannot diffuse into the channels at this temperature. This highly selective adsorption of H_2O over others is attributed to the presence of the narrow pore size (2.0 × 2.8 Å) of **2**, which is very close to the kinetic diameter of H_2O (2.75 Å) and significantly smaller than that of CH_3OH (3.8 Å), CH_3CH_2OH (4.3 Å), and N_2 (3.64 Å) and does not permit these molecules access to the channels.[21] It should be noted that **2** exhibits a highly selective adsorption of water molecules over N_2, CH_3OH, and CH_3CH_2OH, which could be used as a sensor for water molecules with a clear color change.

Magnetic Properties of 1 and 2. The temperature dependencies of magnetic susceptibilities of **1** and **2** were investigated from 300 to 1.8 K with an applied magnetic field of 2000 Oe. The χ_M and $\chi_M T$ vs T curves for **1** and **2** are shown in Figure 5. The center to center distances between the two trinuclear SBUs are long, for example, 9.51, 9.05, and 5.66 Å separated by L^- and 8.55 Å separated by $BTEC^{4-}$ in **1**. Therefore, the magnetic interactions between the adjacent trinuclear SBUs can be ignored, and the interactions can be considered to occur between the two adjacent metal ions bridged by carboxylate groups within the SBU. As is known, the magnetic analysis for the Co(II) complexes is rather complicated because of its spin−orbital coupling, and some approximate methods are applied to analyze the magnetic interactions between the Co(II) ions.[22] For **1**, the $\chi_M T$ value at 300 K is 8.76 emu K mol^{-1}, which is much higher than the sum of three isolated spin-only Co(II) ions of 5.63 emu K mol^{-1} with $g = 2.0$ and $S = 3/2$, ascribing to the contribution of

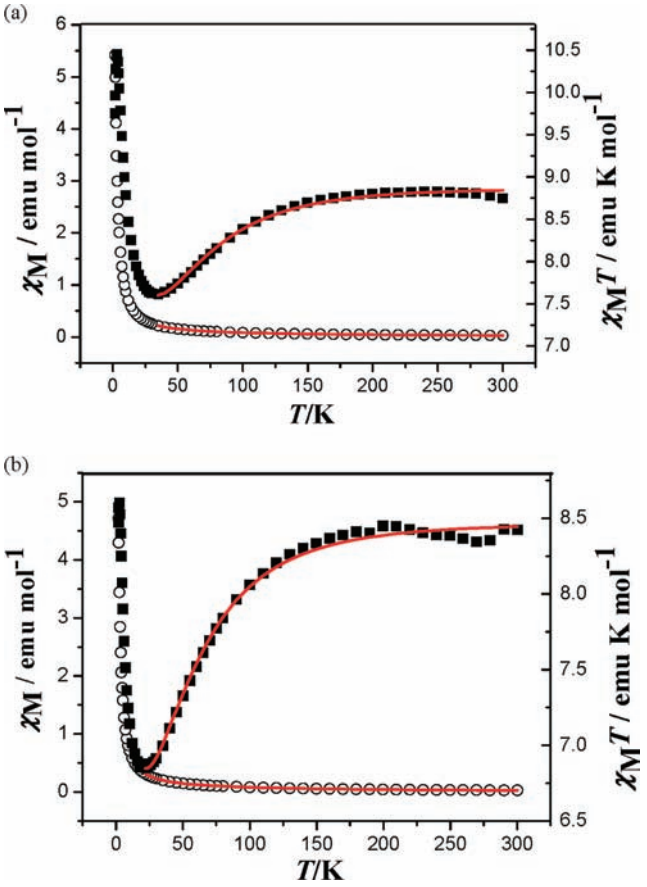

Figure 5. Temperature dependencies of magnetic susceptibility χ_M (○) and $\chi_M T$ (■) for **1** (a) and **2** (b). The solid lines represent the fitted curves.

Co(II) ions (Figure 5a). Similar to the magnetic behavior of other reported Co(II) complexes, the $\chi_M T$ value of **1** slowly decreases upon cooling to 33 K, which is a typical manner of spin−orbit coupling and is mainly due to the single-ion behavior of Co(II).[23] However, the $\chi_M T$ value has an upturn below 33 K, and $\chi_M T$ reaches a maximum of 10.47 emu K mol^{-1} at 3 K, indicating that the ferromagnetic coupling between Co(II) ions occurs in this system and is strong enough to compensate for the single-ion behavior resulting from spin−orbital coupling. The succedent decrease in the $\chi_M T$ vs T curve of **1** should be derived from the inter-Co(II) ions' antiferromagnetic interactions and/or zero field splitting (ZFS). Factually, the overall tendencies in the plot of $\chi_M T$ vs T exhibit the mutual competition between the ferromagnetic coupling and single-ion behavior of Co(II) ions.

An attempt was made, through an expression for the $S = 3/2$ system with eqs 1−4, for **1** to fit the magnetic data above 33 K in order to evaluate dominant zero field splitting effects, D, and the magnetic coupling (zJ) between the neighboring Co(II) centers linked by oxygen atoms, and the interactions between the two terminal Co(II) centers within the SBU were omitted:

$$\chi_{\parallel} = \frac{Ng^2\mu_B^2}{k_B T} \frac{1 + 9\, e^{-2D/k_B T}}{4(1 + e^{-2D/k_B T})} \quad (1)$$

(18) (a) Vishnyakov, A.; Ravikovitch, P. I.; Neimark, A. V.; Bulow, M.; Wang, O. M. *Nano Lett.* **2003**, *3*, 713. (b) Lee, J. Y.; Jagiello, J. *J. Solid State Chem.* **2005**, *178*, 2527.

(19) (a) Zeng, M. H.; Hu, S.; Chen, Q.; Xie, G.; Shuai, Q.; Gao, S. L.; Tang, L. Y. *Inorg. Chem.* **2009**, *48*, 7070. (b) Jiang, J. J.; Li, L.; Lan, M. H.; Pan, M.; Eichhöfer, A.; Fenske, D.; Su, C. Y. *Chem.—Eur. J.* **2010**, *16*, 1841.

(20) (a) Sing, K. S. W. *Pure Appl. Chem.* **1982**, *54*, 2201. (b) Rowcell, J. L. C.; Eckert, J.; Yaghi, O. M. *J. Am. Chem. Soc.* **2005**, *127*, 14904. (c) Xu, J.; Bai, Z. S.; Chen, M. S.; Su, Z.; Chen, S. S.; Sun, W. Y. *CrystEngComm* **2009**, *11*, 2728. (d) Liu, B.; Shiyama, H.; Akita, T.; Xu, Q. *J. Am. Chem. Soc.* **2008**, *130*, 5390.

(21) (a) Coriani, S.; Halkier, A.; Rizzo, A.; Ruud, K. *Chem. Phys. Lett.* **2000**, *326*, 269. (b) Cheon, Y. E.; Suh, M. P. *Chem.—Eur. J.* **2008**, *14*, 3961. (c) Hazra, A.; Kanoo, P.; Mohapatra, S.; Mostafa, G.; Maji, T. K. *CrystEngComm* **2010**, DOI: 10.1039h/b924511a.

(22) (a) Zhang, S. H.; Song, Y.; Liang, H.; Zeng, M. H. *CrystEngComm* **2009**, *11*, 865. (b) Zeng, M. H.; Yao, M. X.; Liang, H.; Zhang, W. X.; Chen, X. M. *Angew Chem. Int. Ed.* **2007**, *46*, 1832. (c) Jia, H. P.; Li, W.; Ju, Z. F.; Zhang, J. *Dalton Trans.* **2007**, 3699.

(23) Sun, H. L.; Wang, Z. M.; Gao, S. *Inorg. Chem.* **2005**, *44*, 2169.

$$\chi_{\perp} = \frac{Ng^2\mu_B^2}{k_B T} \frac{4 + (3k_B T/D)(1 - e^{-2D/k_B T})}{4(1 + e^{-2D/k_B T})} \quad (2)$$

$$\chi' = \frac{\chi_{||} + 2\chi_{\perp}}{3} \quad (3)$$

$$\chi = \frac{\chi'}{1 - \left(\frac{2zJ}{Ng^2\mu_B^2}\right)\chi'} \quad (4)$$

where N is Avogadro's number, μ_B is the Bohr magneton, k_B is Boltzmann's constant, and g is the Lande g value. The best fit in the range of 33−300 K was obtained with values of $g = 2.50$, $D = 80.15$ cm^{-1}, and $zJ = 0.42$ cm^{-1}.[24] The agreement factor R, defined as $\sum[(\chi_M T)_{obsd} - (\chi_M T)_{calcd}]^2/\sum(\chi_M T)^2$, is equal to 8.50×10^{-4}.

Furthermore, the field dependence of the magnetizations of **1** at 1.8 K shows a nearly linear increase below 10 kOe and reaches a value of 8.21 Nβ at 70 kOe (Figure S7, Supporting Information). This value is less than the expected saturation value of 9 Nβ for the Co^{II}_3 cluster with $S = 3/2$ and $g = 2$, which indicates the possible existence of $S = 1/2$ components in the Kramers doublets formed by zero-field splitting.[25]

Similarly, the magnetic measurements for the dehydrated product **2** show that complex **2** has similar magnetic property as **1** (Figure 5b and Figure S8, Supporting Information). The $\chi_M T$ value at 300 K is 8.42 emu K mol^{-1}. The upturn was found at 22 K and then reached a maximum of 8.61 emu K mol^{-1}. The same eqs 1−4 used for **1** were used to fit the data between 22 and 300 K for complex **2** and obtained values of $g = 2.45$, $D = 65.38$ cm^{-1}, and $zJ = 0.75$ cm^{-1} [$R = 1.31 \times 10^{-3}$].

Comparing the fitting results of **1** and **2**, the values of D and zJ decreased and increased upon dehydration, respectively, which is consistent with the structural changes between **1** and **2**. The distances of Co1−Co2 are 3.08 Å in **1** and 3.04 Å in **2**. The shortened distance between Co1 and Co2 in dehydrated **2** leads to the magnetic coupling interaction (zJ) being stronger and the zero-field splitting effect (D) being weaker.

Conclusions

The 3D **tfz-d** topological coordination polymer based on Co(II), 3,5-di(imidazol-1-yl)benzoic acid (HL), and 1,2,4,5-benzenetetracarboxylic acid (H_4BTEC) shows interesting SCSC transformations and reversible dehydration and rehydration phenomena. The dehydrated complex has highly selective adsorption of water molecules over N_2 and other solvent vapors accompanying a color change, which may be used as a sensor for water molecules. The results of the present study provide a nice example of PCPs not only with high stability and SCSC transformation but also with interesting properties of highly selective sorption and sensory for specific molecules.

Acknowledgment. This work was financially supported by the National Natural Science Foundation of China (Grant nos. 20731004 and 21021062) and the National Basic Research Program of China (Grant nos. 2007CB925103 and 2010CB923303).

Supporting Information Available: X-ray crystallographic file in CIF format, crystal structure (Scheme S1, Figures S1 and S2), TGA (Figure S3), PXRD (Figure S4), solid state UV−visible spectra (Figure S5), N_2 adsorption isotherm (Figure S6), magnetic data (Figures S7 and S8). This information is available free of charge via the Internet at http://pubs.acs.org.

(24) (a) Marshall, S. R.; Rheingold, A. L.; Dawe, L. N.; Shum, W. W.; Kitamura, C.; Miller, J. S. *Inorg. Chem.* **2002**, *41*, 3599. (b) Duran, N.; Clegg, W.; Cucurull-Sanchez, L.; Coxall, R. A.; Jimenez, H. R.; Moratal, J. M.; Lloret, F.; Gonzalez-Duarte, P. *Inorg. Chem.* **2000**, *39*, 4821. (c) Nelson, D.; Haar, L. W. T. *Inorg. Chem.* **1993**, *32*, 182.

(25) Kahn, O. *Molecular Magnetism*; VCH: Weinheim, Germany, 1993.